Study on Active Filtering of Current Harmonics Content in Public Lighting Systems

by

Pablo José Quintana Barcia

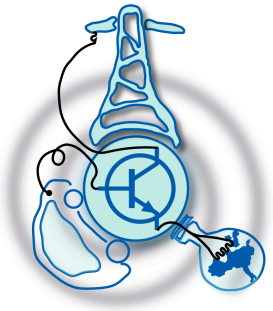

Submitted to the Department of Electrical Engineering, Electronics, Computers and Systems
in partial fulfillment of the requirements for the degree of
Master of Electrical Energy Conversion and Power Systems
at the
UNIVERSIDAD DE OVIEDO
June 2013

Author .....

Certified by .....
Jorge García García
Professor at University of Oviedo
Thesis Supervisor

Certified by .....
Josep María Guerrero Zapata
Professor at Aalborg University
Thesis Supervisor

Study on Active Filtering of Current Harmonics Content in Public Lighting Systems

by

Pablo José Quintana Barcia

Submitted to the Department of Electrical Engineering, Electronics, Computers and Systems
on June 24, 2013, in partial fulfillment of the
requirements for the degree of
Master of Electrical Energy Conversion and Power Systems

Abstract

This Master Thesis is intended to propose a methodology to improve the line current THD of a given distribution line configuration, with multiple non-linear loads (in this case conventional line frequency public lighting systems). The control scheme avoids the use of current sensors, aiming for a low-cost implementation of the algorithm. The implementation of these active filters has been considered for a case of study of correction of the harmonic content generated by a given number of 150W HPS lamps. In addition to the HPS lamp, each lamppost has certain microgeneration capability, by means of a dedicated solar PV panel. In order to compare, different control schematics for the active filter would be studied as part of the internship at the Microgrid Lab of the Department of Energy Technology at Aalborg University in Denmark: two power converters for single-phase microgrids in dq and $\alpha\beta$ reference frame will be evaluated for the use in the proposed active filter. The final objectives are the following:

1. Build a complete model in Matlab/Simulink of the initial public lighting system.
2. Develop a control algorithm for compensation of the line current harmonics of the system.
3. Integrate both the original lighting system and the active filtering system, to attain current harmonics compensation
4. Establishing the limits for the current compensation as a function of the system constraint
5. Evaluate different control schematics for acting as Active Filter connected to the grid.

Thesis Supervisor: Jorge García García
Title: Professor at University of Oviedo

Thesis Supervisor: Josep María Guerrero Zapata
Title: Professor at Aalborg University

Acknowledgments

This work has been supported by the Spanish Government, Innovation and Science Office (MICINN), under research grant no. DPI-2010-15889, Project "Enerlight", by the European Union through the ERFD Structural Funds (Fondos FEDER) and also under the subprogram grant FPI-MICINN, no. BES-2011-047863.

Contents

List of Figures

List of Tables

Glossary

AC	Alternating Current
AF	Active Filter
BPF	Bandpass filter
CM-VSC	Current Mode-Voltage Source Converter
DC	Direct Current
DSP	Digital Signal Processor
FFT	Fast Fourier Transformation
HID	High-Intensity Discharge
HPS	High-Pressure Sodium
LED	Light-Emiting Diode
PCC	Point of Common Coupling
PI	Proportional-Integral
PR	Proportional-Resonant
PV	Photovoltaic
PWM	Pulse-Width Modulation
THD	Total Harmonic Distorsion
VSC	Voltage Source Converter

$\alpha\beta$	Stationary reference frame
bw	Bandwidth
dq	Synchronous reference frame
ε	Error
$\varepsilon_{V_{PCC}}$	Error of the voltage at the PCC between the 1^{st} harmonic

	and the whole harmonic content
F	Farads
H	Henries
i_{LINE}	Current through the line
i_{LOAD}	Current through the load
i_{BAL}	Current of the converter
K_1	Negative admittance of the load
L_G	Inductance of the line from substation to PCC
L_L	Inductance of the line from PCC to loads
R_G	Resistance of the line from substation to PCC
R_L	Resistance of the line from PCC to loads
ω	Frequency in rad/s
Ω	Ohm
θ_e	Angle of synchronization
V_G	Grid voltage
V_{PCC}	Voltage at the point of common coupling
Z_{LOAD}	Impedance of the load

Chapter 1

Introduction

Energy efficiency in lighting applications is a crucial component of the response to climate change. A considerable amount of energy is wasted through inefficient lighting from many sources across the world, including street lighting, commercial, domestic, and office lighting systems. Nearly all of the greenhouse gas emissions from the residential and commercial sectors can be attributed to energy use in buildings. Lighting accounts for about 11% of all the use of energy in residential energy consumption and 18% in commercial buildings [1].In recent years, high frequency electronic ballasts are increasingly used to drive discharge lamps or LED lamps in lighting applications. This replacement began to occur because electronic ballasts present less weight and less volume, besides having an efficiency of about 75% while the conventional electromagnetic ballasts present an efficiency of about 50% maximum [2]. Another benefit of using electronic ballasts is the power factor correction applied to each load (lamps or sets of lamps). In large electrical plants, this approach eliminates the use of big capacitor banks for power factor correction of the whole system [2].

However, currently a number of public lighting systems, based on line frequency conventional electromagnetic ballast are still in use [2–5]. This issue implies high current distortion and current harmonics flowing through distribution lines. These ballasts are formed by a high inductor in series with the lamp, plus a capacitor for improving power factor in the ballast.

The final current drawn by those conventional ballasts has a high THD and sig-

nificant current harmonics content. The lower frequencies (3^{rd}, 5^{th}, 7^{th}...) contain a considerable amount of energy. Potential problems directly related to excessive harmonic currents in the power system are [6]:

- Excessive heating of conductors due to circulating harmonic currents throughout the system.
- Overheating of transformer due to harmonic currents, insulation damage and failure.
- Intermittent electrical noise from connections loosened by thermal cycling.
- Voltage distortion which implies computer ride through capability.
- Power factor correction capacitor failure.

1.1 State of the art of Active Filters

The Active Filter (AF) technology is now mature for providing compensation for harmonics, reactive power, and/or neutral current in AC networks. It has evolved in the past quarter century of development with varying configurations, control strategies, and solid-state devices. AF's are also used to eliminate voltage harmonics, to regulate terminal voltage, to suppress voltage flicker, and to improve voltage balance in three-phase systems. This wide range of objectives is achieved either individually or in combination, depending upon the requirements and control strategy and configuration which have to be selected appropriately [6].

There is a large number of publications covering the power quality survey, measurements, analysis, cause, and effects of harmonics and reactive power in the electric networks and several methods to reduce current harmonics content [7–19]. The increased severity of this kind of pollution in power networks has attracted the attention of power electronics and power system engineers to develop dynamic and adjustable solutions to the power quality problems [15–19]. Different topologies to correct the current harmonics distortion can be found in the literature [7–19]. The main schemes

can be classified based on converter type, topology, and the number of phases [6]. Basically, there are two types of converters used in the development of AF. In Figure 1-1(a), the current-fed Pulse Width Modulation (PWM) inverter bridge structure is shown. It behaves as a non-sinusoidal current source to meet the harmonic current requirement of the nonlinear load [6]. The other converter used as an AF is a voltage-fed PWM inverter structure, as it is shown in Figure 1-1(b). It has a self-supporting DC voltage bus with a large capacitor. It has become more dominant, since it is lighter, cheaper, and expandable to multilevel and multistep versions, to enhance the performance with lower switching frequencies [6]. It is worth noting that being controller with an inner current control loop, it behaves as a current source from the point of common coupling (PCC) point of view.

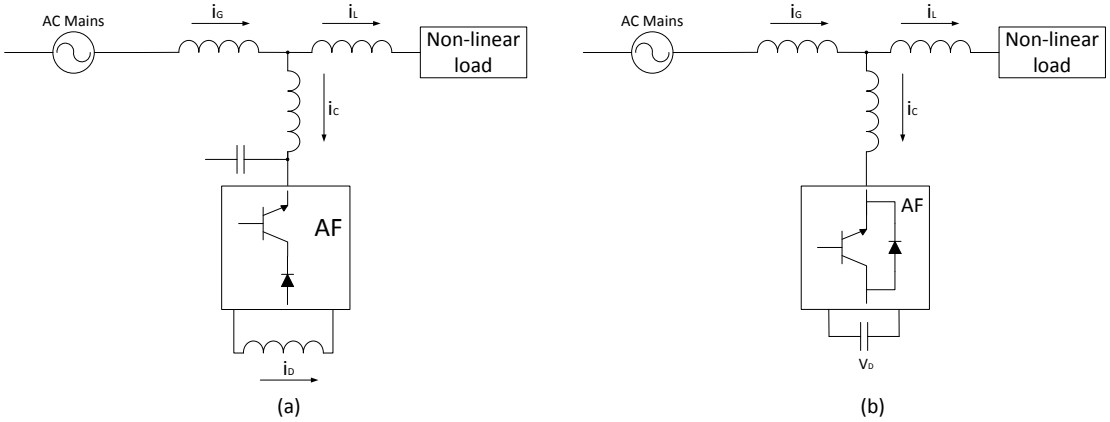

Figure 1-1: (a) Current-fed-type AF (b) Voltage-fed-type AF

These techniques [12–14], [17] for multiple non-linear loads used to have an active filter based on a single-phase inverter with four controllable switches, a standard H-bridge inverter [6] or a three-phase one [18], [19]. The AC side of the inverter is connected in parallel with the other nonlinear loads through a filter inductance. The DC side of the inverter is connected to a filter capacitor [6]. The inverter switches are controlled to shape the current through the filter inductor such that the line current, assuming no reactive power is required, is in phase with, and of the same shape as, the input voltage [6]. All these topologies have in common the line current measurement [7–18]. The necessary sensors for a proper current measurement with enough

bandwidth implies a significant cost over the full system and reduced reliability. On the other hand, for some reasons, sometimes it is difficult to access to the current measurement, for example, in the case of streetlamps. In this Master Thesis, a system of current harmonics compensation without current sensing is proposed and tested by simulations.

Chapter 2

Model of the initial public lighting system

2.1 Lighting systems based on electromagnetic ballasts

Figure 2-1 shows a basic diagram, considering a case of study, from the substation to the load that represents how they will be connected. The load in the simulation represents 250 ballasts with their respective lamps, in this case 150W High-Pressure Sodium (HPS) Lamps.

These 250 ballast and lamps simulate a group of streetlamps (see Figure 2-2) with a solar PV panel and a Savonius wind turbine providing energy that could be used to feed the lamp or to be injected in the grid. As the converter topology would be an H-bridge, the active and reactive power are fully decoupled, so the harmonic compensation is feasible. Every ballast of each streetlamp would have an electronic ballast to develop this aim, but in this thesis, a unique equivalent system, with the total rated power is considered (e.g. 250x150W) in order to simplify the problem.

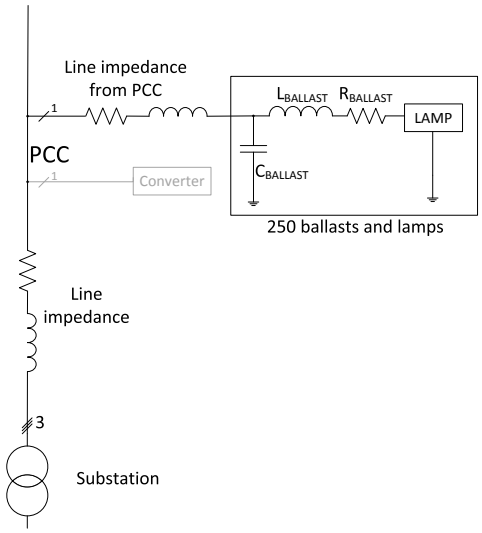

Figure 2-1: Basic scheme of the simulation

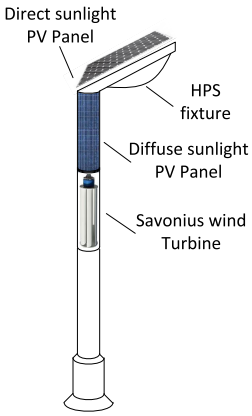

Figure 2-2: Example of public lighting post based on photovoltaic modules and small wind generators, incorporated into the fixture aesthetics

2.2 Model of the electromagnetic ballast

The model of the conventional low frequency electromagnetic ballast and the 150W HPS lamp was taken from real devices and built in Simulink. This model is needed to simulate the line current demanded by the real loads, which would be several conventional streetlamps, and then study how to compensate its effect in the grid and possible solutions.

From the real ballast and lamp, real data was taken and it is summarized in Table 2.1:

Table 2.1: Real ballast information

Ballast current (A)	Ballast voltage (V)	Rballast (Ω)	Lballast (mH)	Cballast(μF)
1	320	5.5	325	20

Table 2.2: Group of 50 ballast information

Rmodel (Ω)	Lmodel (mH)	Cmodel(mF)
0.11	6.50	1.00

And from Table 2.1, the model can be implemented, taking into account that every group of lamps is formed by 50 elements, so the values of each group are gathered in Table 2.2:

The model of this group of ballast is represented in Figure 2-3:

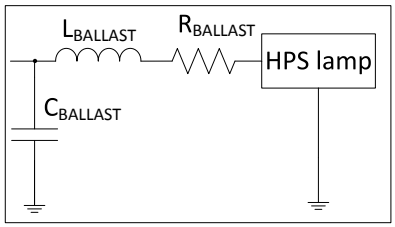

Figure 2-3: Implemented model of the ballast

2.3 Model of the HPS lamp

2.3.1 Previous models

In [20–22] are presented different techniques and models for HPS lamps. The behavior of these models is accurate but generally complex to develop.

Much effort has been devoted to the development of sophisticated High-Intensity Discharge (HID) lamp models based on advanced diagnostic techniques in the last few decades. However, most of these models are complicated and there is a lack of practical HID lamp models that are accurate enough and yet can be easily implemented in

circuit simulation software. In fact, HID lamps are extremely complex devices, which have many variables and parameters to be determined for optimum performance.

In [20], based on the physical laws of plasma discharge, a simplified but accurate model is presented. Figure 2-4 shows the model in PSpice of the HID model.

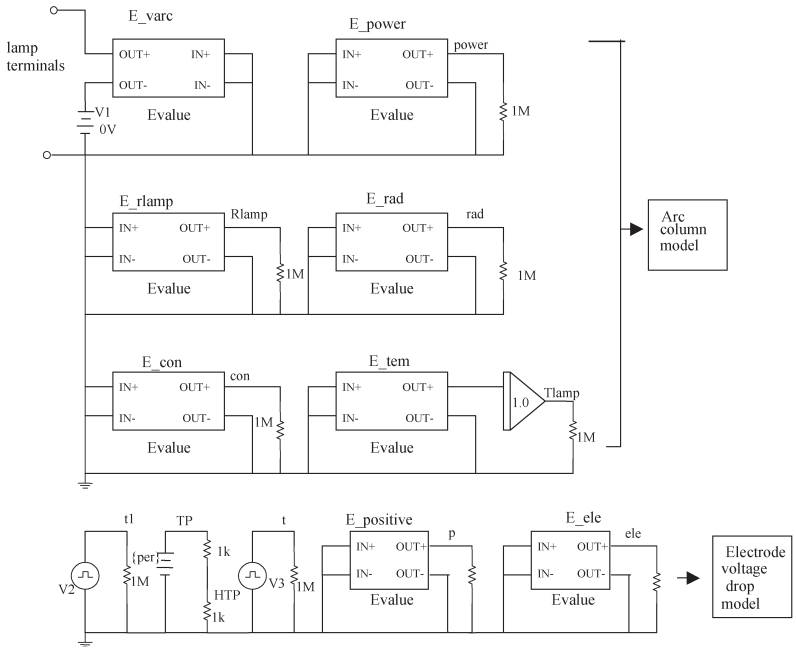

Figure 2-4: PSpice HID lamp model structure [20]. *Permission to include it granted.*

That model did not require data from lamp manufacturers. Its parameters were determined from external measurements of the lamps under low-frequency operation only, but the model is accurate for both low and high frequency operations. The lamp model is based on the fundamental physical processes inside the arc column and the electrode sheath. In Figure 2-5 are shown the experimental and PSpice simulated lamp voltage and current waveform of 50W Philips mercury lamp at 50Hz operating frequency [20].

On the other hand, in [21], another different kind of model is presented: a non-linear model of HID lamps based on electrical variables. The proposal, oriented to the engineering area, has a special application for the design of electronic ballast. Parameters were obtained from straightforward measurement of electrical variables as power, current, and voltage in the lamp. The lamp resistance was obtained as a

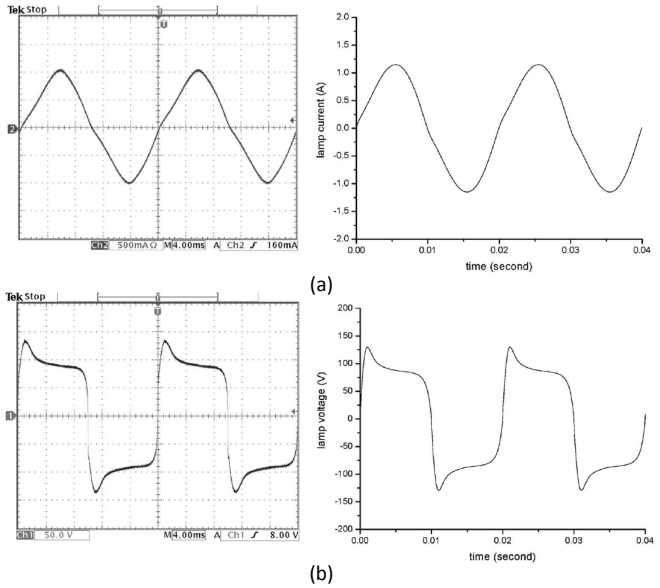

Figure 2-5: (a) Experimental lamp current wave form and PSpice simulated lamp current wave form [20]. (b) Experimental lamp voltage waveform and PSpice simulated lamp voltage waveform [20]. *Permission to include it granted.*

function of electrical power. This model takes into account some important dynamic behaviors of HID lamps, which are normally omitted in some other models suggested in literature nowadays. In Figure 2-6 can be seen the proposed model implemented in Simulink.

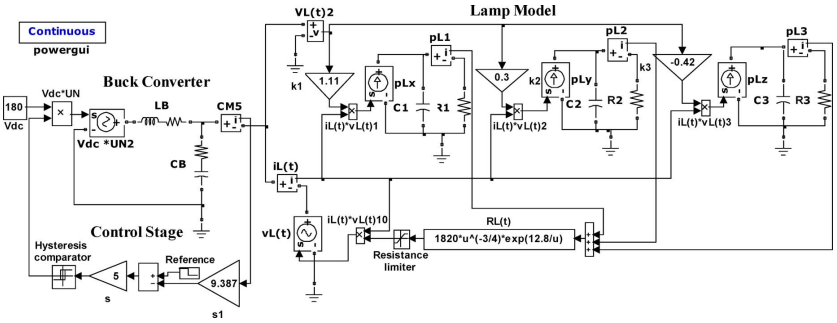

Figure 2-6: Proposed model implemented in Simulink. [21]. *Permission to include it granted.*

Figure 2-7 shows a current-step test from a low to a high current value; this test is useful in order to demonstrate that this model works fine for different operation points.

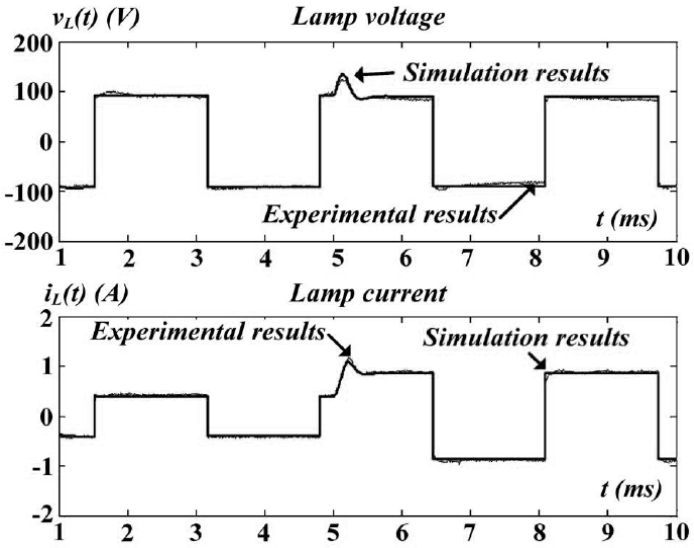

Figure 2-7: Step-up test from a low current value to a high current value [21]. *Permission to include it granted.*

2.3.2 Developed model

In this thesis, a simpler model was done in order to be easy to simulate in multiple simulation platforms (PSpice, PSIM, Matlab-Simulink, dSPACE). However, despite its simplicity, the information given about the harmonics generation in the grid is reliable and its behavior is precise in comparison with the real values. The lamp model is based on the voltage-source behavior of the lamp discharge at low frequency. Two zener diodes in anti-series configuration model the basic behavior of the discharge, being the zener voltage the arc voltage of the lamp. Two exponential curves used to model the time constants of the re-ignition peak have also been added to this basic model. As a result, the final lamp model is presented in Figure 2-8.

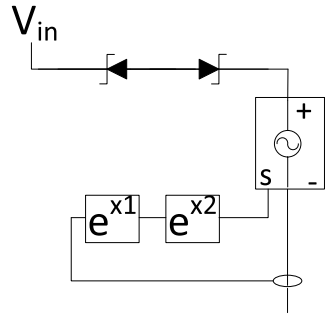

Figure 2-8: Model of the lamp.

In Figures 2-9 and Figures 2-10 is shown the data obtained from the real model, which are the real measurements and the averaged ones, and the characteristic curve I-V of the lamp.

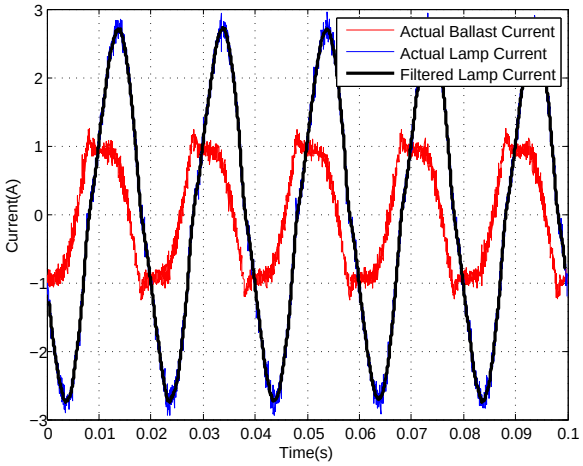

Figure 2-9: Ballast and lamp currents.

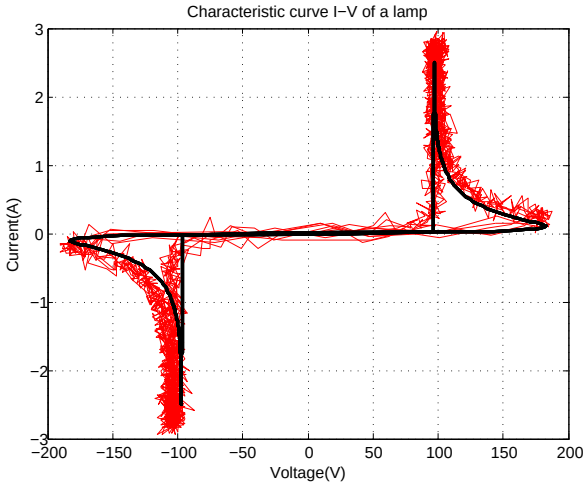

Figure 2-10: Characteristic curve I-V of the lamp. Red: real measurements. Black: model results.

In Figure 2-11, both the real data taken from the lamp and the results of the model can be seen. This model can be used in the future hence it works as a real lamp. On the other hand, Figure 2-12 shows the total current demanded in the case of study of Figure 2-1. It can be seen how this current waveform is not sinusoidal, what yields to large harmonic content. The THD of this current in Figure 2-12 was

calculated and the result was a 21.34% which is a value clearly out of the reasonable limits of the THD.

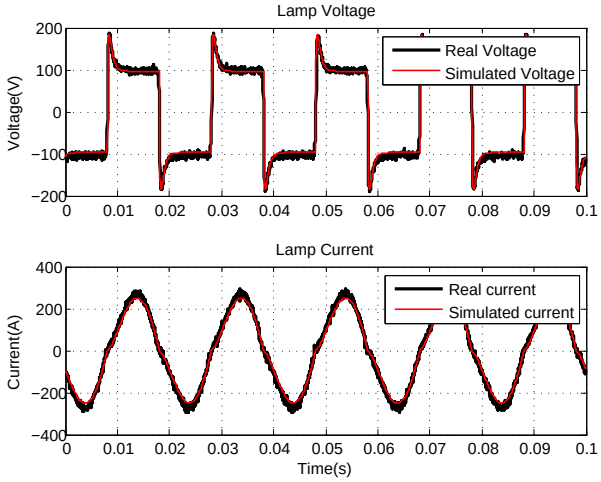

Figure 2-11: Comparison between real data (black) and the model (red).

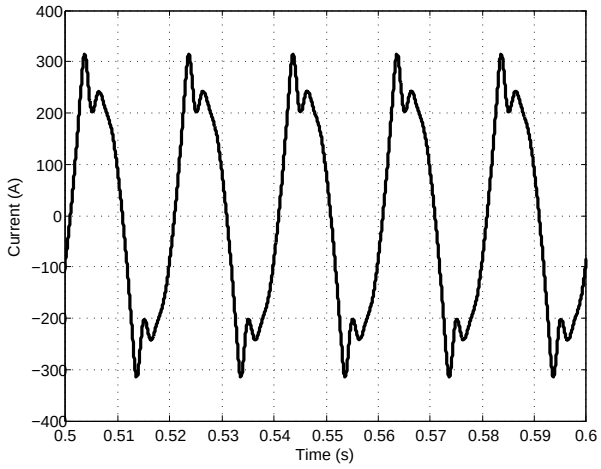

Figure 2-12: Current demanded by the loads (250 ballasts).

2.4 Complete model in Matlab/Simulink of the initial public lighting system

The model of the public system was built using Simulink and the SimPowerSystems library. In Figure 2-13 can be seen the whole electric diagram, combining together

the electromagnetic ballasts and the model of the lamps (Figure 2-14) previously commented.

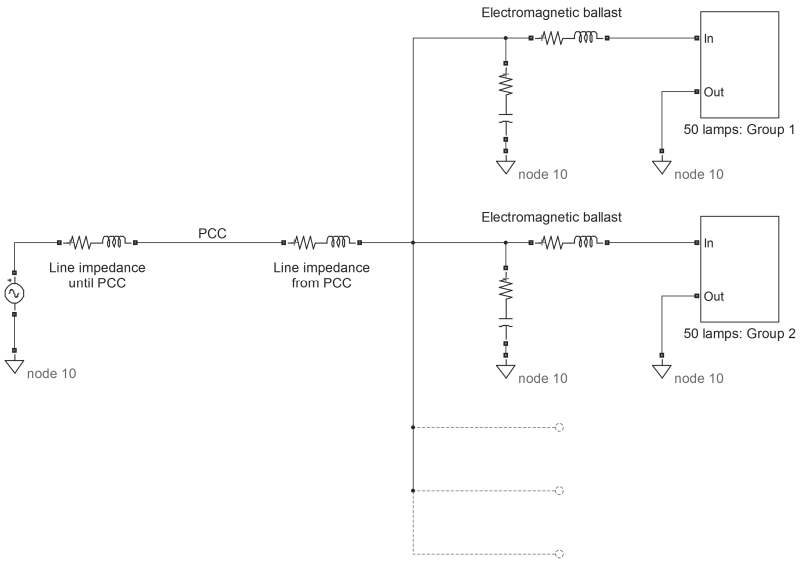

Figure 2-13: Basic diagram in Simulink.

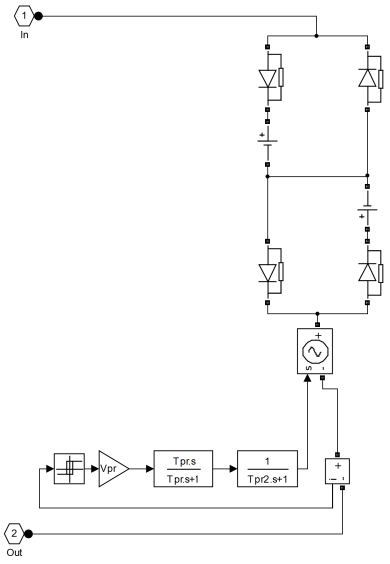

Figure 2-14: Simulink model of the HPS lamp.

Chapter 3

Proposed control strategy

In order to mitigate the harmonic content of the line current of a distribution line like the one shown in Figure 2-1, a technique based on measuring the voltage at the PCC is proposed. The proposal aims not only to provide a high power factor correction, but also to reduce the effect of the remaining conventional ballasts of an existing line of 250 HPS lamps of a rated power of 150W each one. In fact, a new line of streetlamps fed by renewable energies could be installed in parallel with this ballasts line and using any kind of lightning system without affecting the behavior of the existing harmonic correction converter. The implementation of the proposed method only requires measuring the voltage at the PCC, which is also required for grid synchronization, and removes the need of the current sensor at the line. The harmonic distortion of the PCC voltage is calculated, and a current proportional to this distortion is injected for generating the overall current reference of the system. The avoidance of the line current sensor will decrease in a noticeable way the cabling cost and will increase the reliability of the whole system. Thus, to define the operation of the converter, the reference for the instant input current on the converter must be defined. The procedure for obtaining this reference waveform is shown ahead:

Firstly, based on Figure 3-1, it can be stated that:

$$i_{LINE} = \frac{V_G - V_{PCC}}{s \cdot L_G + R_G} \tag{3.1}$$

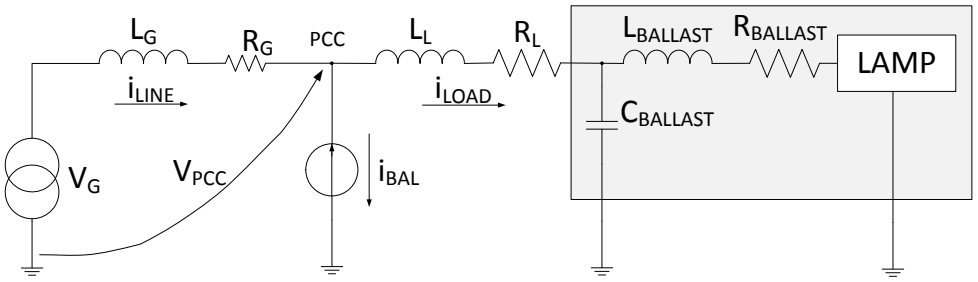

Figure 3-1: Proposed electrical model.

$$V_{PCC} = i_{LOAD} \cdot Z_{LOAD} \tag{3.2}$$

$$i_{LOAD} + i_{BAL} = i_{LINE} \tag{3.3}$$

where Z_{LOAD} is the impedance from the PCC to the lamps, which is not linear, but a combination of the impedance of the ballasts and effect of the lamp.

The currents and voltages can be separated in two components: the fundamental harmonic at 50Hz (x_{y_1}) and the rest of the harmonic content($x_{y_{HF}}$), where x can be the current or the voltage and y, the measurement point: load, PCC or the proposed converter:

$$i_{LOAD} = i_{LOAD_1} + i_{LOAD_{HF}} \tag{3.4}$$

$$i_{BAL} = i_{BAL_1} + i_{BAL_{HF}} \tag{3.5}$$

$$V_{PCC} = V_{PCC_1} + V_{PCC_{HF}} \tag{3.6}$$

The calculation of the first harmonic, at 50Hz, has been done using a resonant filter at 50Hz. The main drawback of this filter is that if a sudden change takes place in the grid frequency, the dynamics of the filter can provide wrong measurements, so it would need to be well designed and optimized.

In order to calculate the current reference and to achieve the final goal, that is having a sinusoidal line current i_{LINE}, (3.3), (3.4) and (3.5) can be combined:

$$(i_{LOAD_1} + i_{LOAD_{HF}}) + (i_{BAL_1} + i_{BAL_{HF}}) = (i_{LINE_1} + i_{LINE_{HF}}) \tag{3.7}$$

3.1 Calculation of the high frequency current reference

In order to enhance the operation of the full system, in (3.7), $i_{LINE_{HF}}$ must be zero, thus we can state that in (3.8) and (3.9) have to be fulfilled:

$$i_{LINE_{HF}} = 0 \tag{3.8}$$

$$i_{LOAD_{HF}} = -i_{BAL_{HF}} \tag{3.9}$$

Combining (3.7), (3.8) and (3.9), we arrive to:

$$i_{LOAD_1} + i_{BAL_1} = i_{LINE_1} \tag{3.10}$$

On the other hand, substituting (3.6) in (3.2):

$$V_{PCC_1} + V_{PCC_{HF}} = i_{LOAD} \cdot Z_{LOAD} \tag{3.11}$$

Including (3.4) in (3.11):

$$V_{PCC_1} + V_{PCC_{HF}} = i_{LOAD_1} \cdot Z_{LOAD} + i_{LOAD_{HF}} \cdot Z_{LOAD} \tag{3.12}$$

First harmonic component and the high frequency terms can be splitted in:

$$\begin{cases} V_{PCC_1} = i_{LOAD_1} \cdot Z_{LOAD} \\ V_{PCC_{HF}} = i_{LOAD_{HF}} \cdot Z_{LOAD} \end{cases} \tag{3.13}$$

where Z_{LOAD} is not just a lineal impedance and its value changes for each harmonic.

With (3.9) and (3.13), it can be defined:

$$V_{PCC_{HF}} = -i_{BAL_{HF}} \cdot Z_{LOAD} \tag{3.14}$$

And substituting (3.14) in (3.6):

$$\begin{aligned} V_{PCC} - V_{PCC_1} = V_{PCC_{HF}} = -i_{BAL_{HF}} \cdot Z_{LOAD} \Rightarrow \\ \Rightarrow i_{BAL_{HF}} = \frac{-1}{Z_{LOAD}} \cdot (V_{PCC} - V_{PCC_1}) \end{aligned} \tag{3.15}$$

where $V_{PCC} - V_{PCC_1}$ is the difference between the voltage at the PCC and the first harmonic of the same voltage, which will be considered the voltage error, $\varepsilon_{V_{PCC}}$. Besides, $i_{BAL_{HF}}$ will be the high frequency content of current through the converter and Z_{LOAD} the non-linear impedance from the PCC to the lamps. Up to here it has been defined the high frequency term of the current reference that would finally be:

$$i_{BAL_{HF}} = K_1 \cdot \varepsilon_{V_{PCC}} \tag{3.16}$$

being $K_1 = \frac{-1}{Z_{LOAD}}$, the admittance of the load, but like it was commented before, it depends on many factors and change with every harmonic, so it is not easy to determine exactly its value.

3.2 Calculation of the 50Hz current reference

Thus, in order to generate the current reference for the proposed filter, and once the $i_{BAL_{HF}}$ component is calculated, the fundamental component i_{BAL_1} is needed. In order to obtain this value, the following procedure will be done (see Figure 3-2): Once the input power value is known and the PCC voltage is measured, the value of

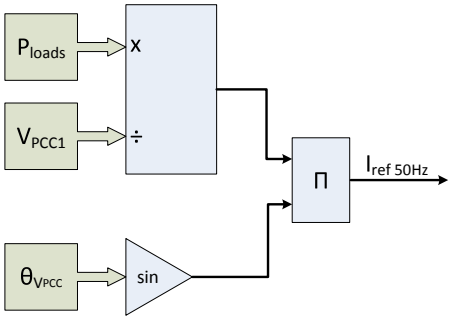

Figure 3-2: Calculus of the 50Hz current reference.

the input current for a unity power factor system can be easily calculated:

$$P_{BAL} = V_{PCC_1} \cdot i_{BAL_1} \cdot \cos\theta \Rightarrow i_{BAL_1} = \frac{P_{BAL}}{V_{PCC_{1\_peak}}} \tag{3.17}$$

where P_{BAL} is the power of the lamps system, to simplify the problem, $V_{PCC_{1\_peak}}$ the peak amplitude of the first harmonic of the voltage at the PCC and i_{BAL_1} the amplitude of first harmonic of the current reference. The phase needed to generate the current reference of the first harmonic is selected as the phase of the fundamental harmonic of the voltage measured at the PCC, as can be seen in Figure 3-2.

Now, the final current reference value can be stated by adding (3.16) and (3.17):

$$i_{BAL_{ref}} = i_{BAL_1} + i_{BAL_{HF}} = i_{BAL_1} + K_1 \cdot \varepsilon_{V_{PCC}} \tag{3.18}$$

Chapter 4

Integration of both systems. Simulations

Instead of the proposed model based on the non-linear impedance of the load, a simplification is here assumed for the initial testing of the method. As it was explained before, knowing the exactly value of K_1 is a tough mission, and the reason is that since it is the admittance from the PCC to the lamps, its value varies between a big range due to the effect of the harmonics. In fact, if it was feasible to know its precise value, it would be hard to calculate and also difficult to implement in a Digital Signal Processor (DSP). Then, Z_{LOAD} term is changed to a gain, thus simplifying the impedance to a resistance and the value is increased above the theoretical one in order to achieve the needed bandwidth for the compensation. Thus this simplification and since (3.18) is based on a proportional gain K_1, the bigger value it gets, the better THD of the line current the system will have because the error is reduced due to it follows (4.1) and Figure 4-1. If a finite K_1 was desired, then a PI controller should be used, but since the signals are not DC, a traditional regulator like a PI would not accomplish the final goal. In this case, thinking in resonant converters would be a better idea. But right now, a first approach based just on a proportional gain will be done.

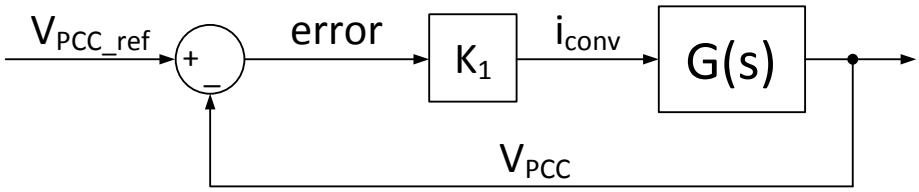

Figure 4-1: Basic diagram of the effect of K_1.

$$\lim_{k \to \infty} \varepsilon = 0 \tag{4.1}$$

Nevertheless, there are some limitations that should be mentioned:

The proposed current controlled converter is basically a low cost electronic ballast, with an input bidirectional PFC stage (i.e. H bridge converter). The measurement needed is the voltage at the PCC, done by a cheap sensor, so the error between the first harmonic and the whole signal should not be zero, thus the control will not work properly. These are limitations for K_1.

Several simulations with different values of the gain K_1 were made, and the main results are summarized in Tables 4.1 and 4.2. These data are graphically summarized ahead. It will be shown the THD value of the current through the distribution line from the substation, the values of the main harmonics of the same current and finally, the error between the 1st harmonic and the whole voltage at the PCC and the rms current through the converter.

It will be shown the THD value of the current through the line, the values of the main harmonics of the same current and finally, the error between the 1^{st} harmonic and the whole voltage at the PCC and the current through the converter. Figures 4-2, 4-3 and 4-4 show graphical representations of the main data of Tables 4.1 and 4.2. As a conclusion, it can be said that the harmonic content has been reduced because the most harmful harmonics, 3^{rd}, 5^{th} and 7^{th}, have been decreased and also the THD of the current through the distribution line decreases continuously for the reason explained before. The more K_1, the more sinusoidal is the current and thus, the lower the THD. If we continued increasing this gain, the error would become almost zero, but it would not represent a real case because the voltage sensor is not so perfect.

Table 4.1: THD and harmonics of the current through the line depending on the different constants (in Amps), error of the voltage at the PCC and Current through the converter

K_1	THD Current	1^{st} harm (A)	3^{rd} harm (A)	5^{th} harm (A)	7^{th} harm (A)	9^{th} harm (A)	$\varepsilon_{V_{PCC}}$ (V)	$I_{conv_{rms}}$ (A)
Off	0.2133	273.1	47.90	26.01	18.77	2.92	2.50	0
0	0.4053	144.59	48.17	26.17	18.84	7.94	2.52	95.70
20	0.2734	136.01	33.28	14.21	7.40	3.71	2.54	101.21
40	0.1924	138.85	24.45	9.30	4.56	2.41	2.45	113.73
60	0.1351	152.97	19.10	6.86	3.29	1.79	2.38	131.12
80	0.0956	175.48	15.57	5.40	2.57	1.42	2.32	151.99
100	0.0691	203.52	13.10	4.45	2.10	1.17	2.29	175.13
120	0.0517	235.56	11.36	3.80	1.79	1.00	2.26	199.88
140	0.0396	270.38	9.99	3.31	1.55	0.87	2.24	225.46
160	0.0311	307.11	8.92	2.92	1.37	0.77	2.22	251.78
180	0.0249	344.45	8.04	2.62	1.23	0.69	2.20	278.71
200	0.0205	382.72	7.36	2.38	1.11	0.63	2.19	305.91

Table 4.2: THD and harmonics of the current through the line depending on the different constants (in % over normalized over the 1^{st} harmonic)

K_1	THD Current	1^{st} harm (%)	3^{rd} harm (%)	5^{th} harm (%)	7^{th} harm (%)	9^{th} harm (%)
Off	0.2133	100	17.54	9.52	6.87	1.06
0	0.4053	100	33.31	18.09	13.02	5.49
20	0.2734	100	24.47	10.44	5.44	2.72
40	0.1924	100	17.60	6.69	3.28	1.73
60	0.1351	100	12.48	4.48	2.15	1.17
80	0.0956	100	8.87	3.07	1.46	0.80
100	0.0691	100	6.43	2.18	1.03	0.57
120	0.0517	100	4.82	1.61	0.75	0.42
140	0.0396	100	3.69	1.22	0.57	0.32
160	0.0311	100	2.90	0.95	0.44	0.25
180	0.0249	100	2.33	0.76	0.35	0.20
200	0.0205	100	1.92	0.62	0.29	0.16

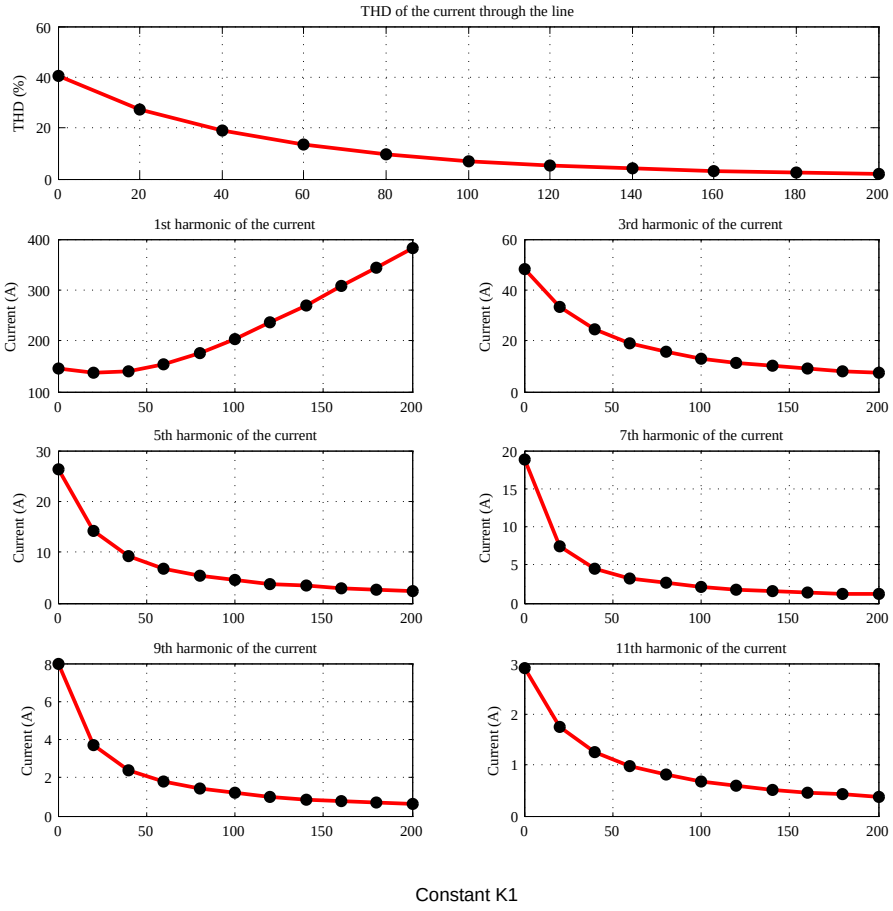

Figure 4-2: Results of Table 4.1.

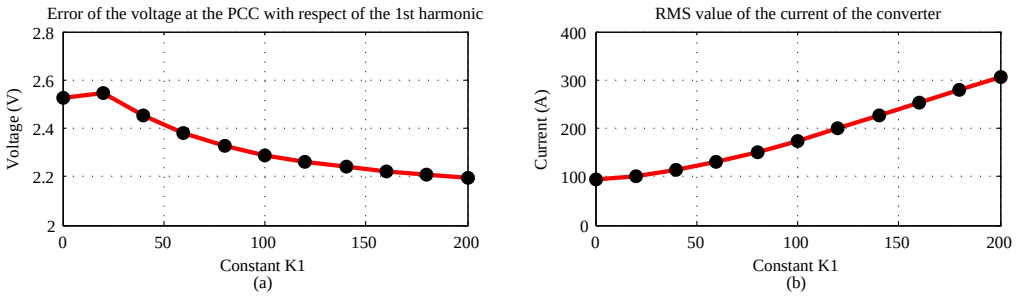

Figure 4-3: (a) Error of the voltage at the PCC. (b) RMS current through the converter.

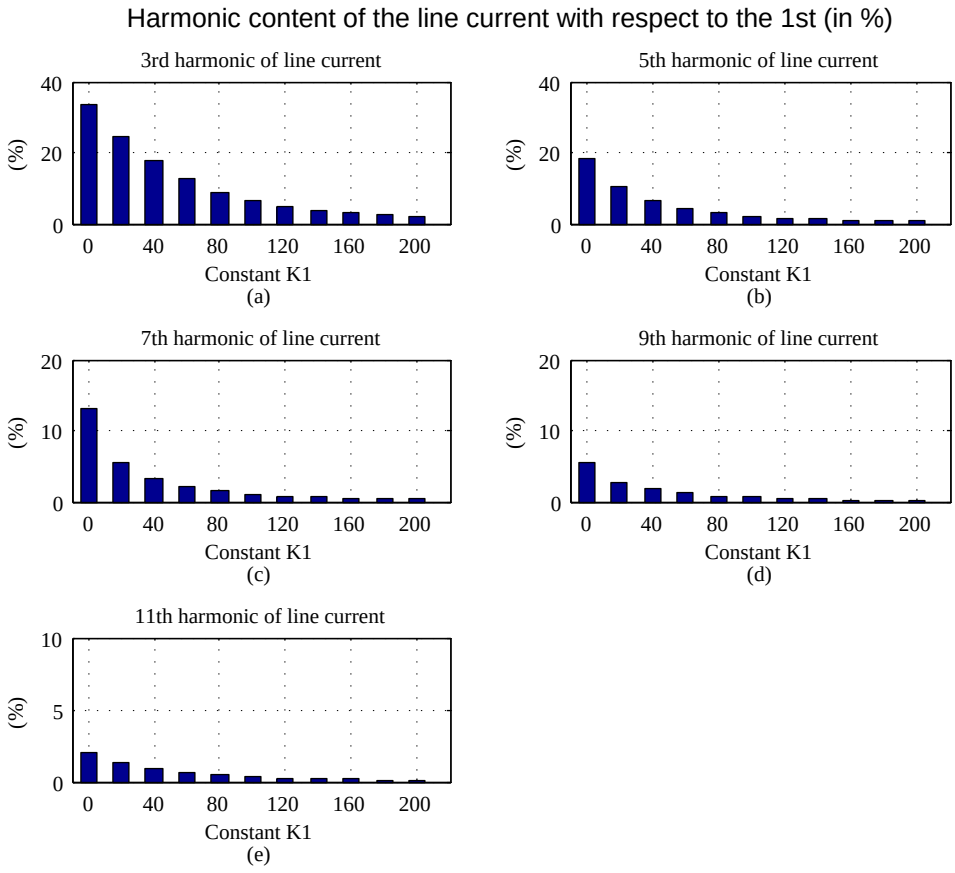

Figure 4-4: Results of Table 4.2

Chapter 5

Selection of an optimal value for K_1 and analysis of the results

In order to show some results is needed to choose a value for K_1. As it was said, according to the simplification of Z_{LOAD} by a gain, the best value of K_1 would be ∞ but it is not feasible. However, a possible value looking at Table 4.1 would be 120, reducing the THD to a 5%. With this value of K_1 it is been reducing the value of the 3^{rd} harmonic in a 13%. That is the reason why we have chosen this constant. There are several options: for example, having a K_1 of 140, the THD is reduced to a 4% instead of the previous 5%, but, on contrary, the 3^{rd} harmonic is not almost decreased with respect the previous case and the current the converter is delivering is bigger in $25A$, so, for a little improvement in the THD, the effort, in terms of current, is huge. The following reveal a comparison of the simulation results between normal operation of the converter, i.e. sinusoidal input current to the ballasts, and the proposed current compensation operation. In Figure 5-1a it can be seen the difference between the first harmonic of the current through the distribution line and the overall current when the converter does not work. In Figure 5-1b, the same plot is repeated for the case the converter is connected with a constant K_1 of 120. It can be seen that the difference is very significant. The following Figure 5-2 shows the difference in the harmonic content of the line current.

In Figure 5-3 is shown the current demanded by the loads (red) and the current

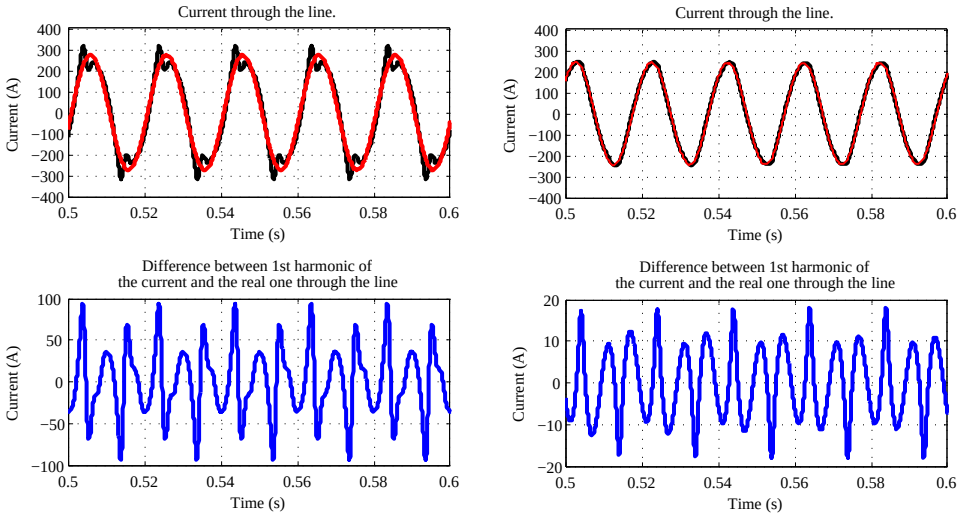

(a) Converter Off (b) Converter On

Figure 5-1: (a) Current through the line and difference with 1st harmonic when the converter is off. (b) Current through the line and difference with 1st harmonic when $K_1 = 120$.

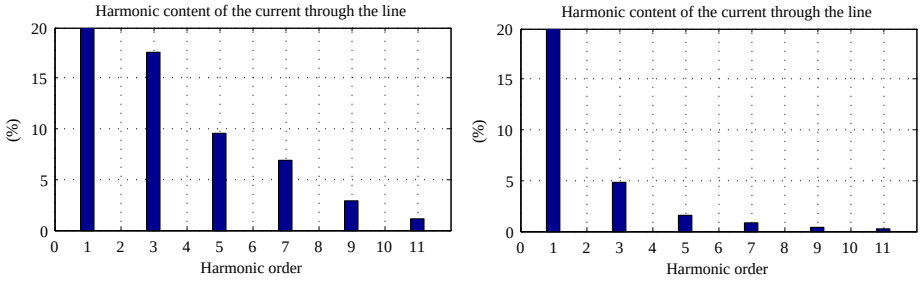

(a) Converter Off (b) Converter On

Figure 5-2: Harmonic content of the current though the line, in %, normalized to the 1^{st} harmonic: (a) When the converter is off. (b) When $K_1 = 120$. The 1^{st} harmonic has a value of 100%

of the converter (black). It is noticeable how the converter tries to correct the peaks of the load current and do it the most sinusoidal it can (Figure 5-1b).

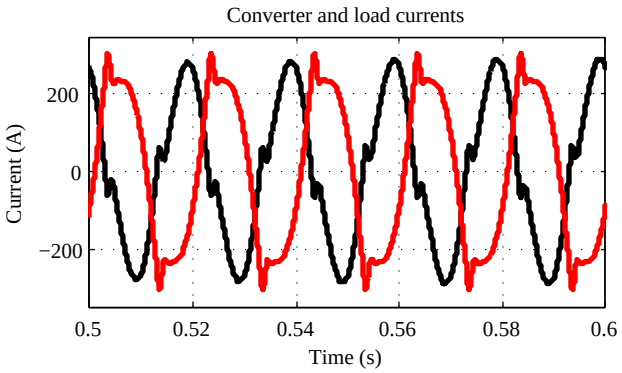

Figure 5-3: Current through the converter (black) and through the load (red).

The following Figures 5-4 and 5-6 show the result of using a lower value of K_1: 80 in this case. It can be appreciated the change in the error between the first harmonic of the current and the real current. In this case, it is bigger than the previous case and it is due to the fact that the amount of current the converter is handling now is lower. It can be seen in Figure 5-6, where the current of the converter is in black. The THD is reduced to a 9.5% in this case. The following Figure 5-5 shows the difference in the harmonic content of the line current.

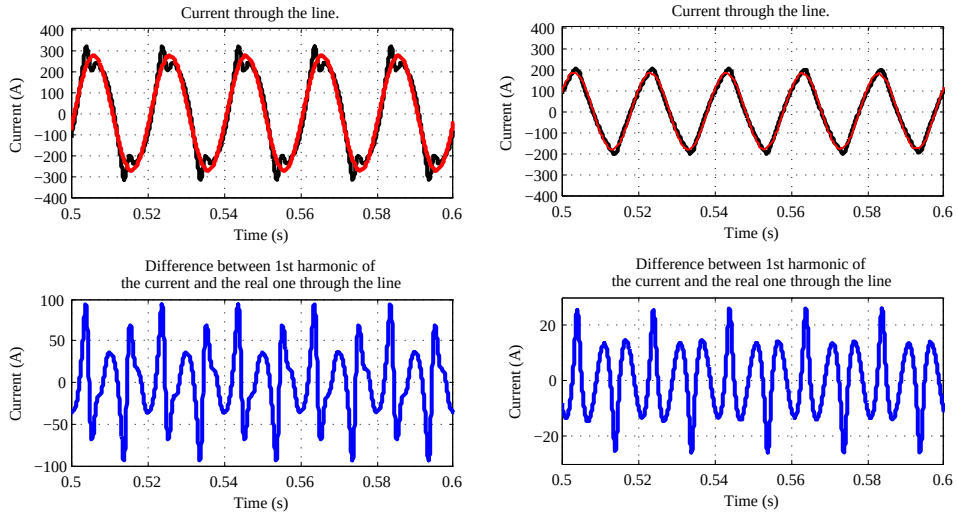

(a) Converter Off (b) Converter On

Figure 5-4: (a) Current through the line and difference with 1st harmonic when the converter is off. (b) Current through the line and difference with 1st harmonic when $K_1 = 80$.

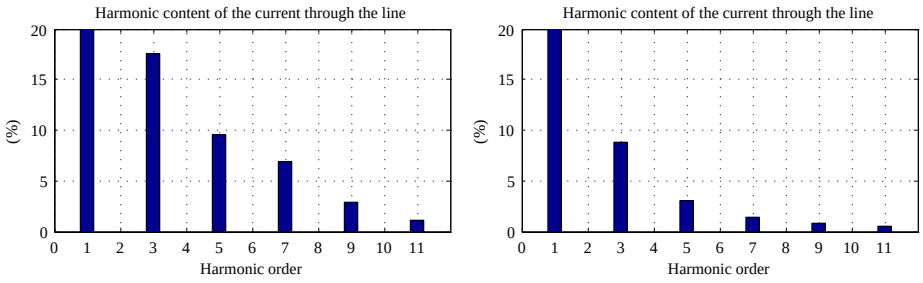

(a) Converter Off (b) Converter On

Figure 5-5: Harmonic content of the current though the line, in %, normalized to the 1^{st} harmonic: (a) When the converter is off. (b) When $K_1 = 80$. The 1^{st} harmonic has a value of 100%

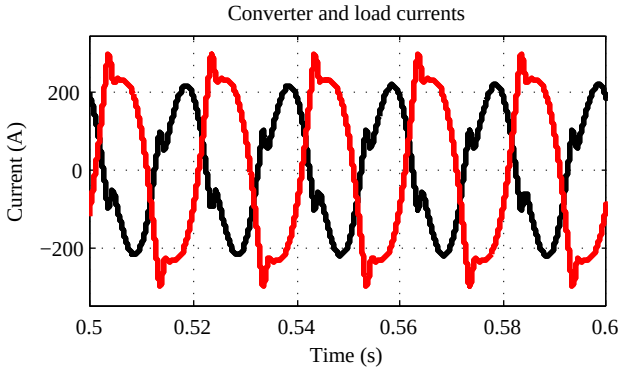

Figure 5-6: Current through the converter (black) and through the load (red).

Chapter 6

Evaluation of different topologies to compensate the production of harmonics by the loads

Until this point, a methodology using only voltage measurements at the PCC was explained. These previous results will be published in the IECON 2013 conference. In order to compare with other techniques and using the equipment of Aalborg University, different simulations were developed.

Before that, it should be explained that as part of the internship at Aalborg University in Denmark, different control schematics for single-phase microgrids, connected to grid and in island mode, were studied. In Figures 6-1 and 6-2 can be seen the two different cases previously mentioned. Each case was operated in two different ways, with and without droop, hence four different simulations were done (all in dq reference frame and also some in $\alpha\beta$):

- Current Mode-Voltage Source Inverter (CM-VSI) grid supporting with droop
- CM-VSI grid feeding
- VSI grid forming with droop
- VSI grid forming without droop

The two first CM-VSI work connected to the grid and the last two VSI, in island mode. CM-VSI control schematics has only one inner current loop but a VSI needs two loops, one for the voltage and another for the current.

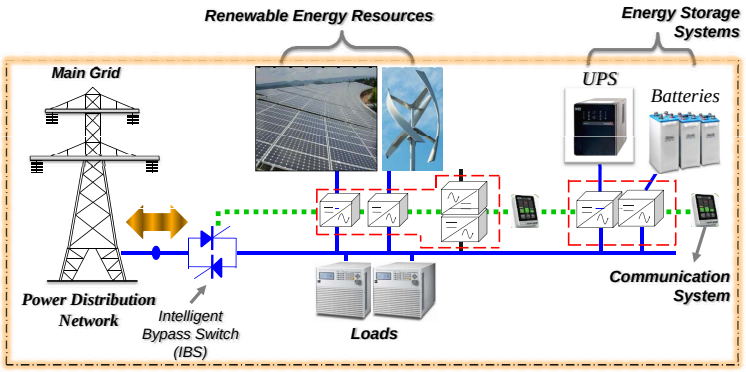

Figure 6-1: Converter (CM-VSI) connected to the main grid [23]. *Permission to include it granted.*

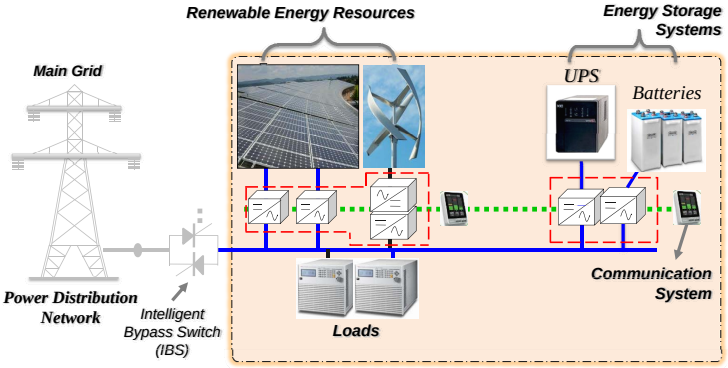

Figure 6-2: Converter (VSI) working in island [23]. *Permission to include it granted.*

However, these considered control schematics are not prepared to improve the harmonic effect of the loads in the line with the actual control strategy. They were designed just to help the grid or to act in island mode when the loads have not a very high harmonic content though. Since explaining how the previous four strategies work is not an objective of this master thesis (more information in [23], [24]), just the part related to harmonic correction will be commented. But previously, it is important to say that, though this work have been done previously in Simulink, the results obtained in the dSPACE (Digital Signal Processing And Control Engineering) environment will be shown, which is also called "Hardware in the loop" due to the fact that the variables

can be changed in real time and its effects are seen also instantaneously.

6.1 Reduction of harmonic content in dq reference frame

The first control schematics thought to correct the harmonic content can be seen in Figure 6-3. It can be observed that there are many band-pass filters (BPF) whose mission is to extract the desired frequencies from the grid current, which would be 150Hz, 250Hz, 350Hz and 450Hz, corresponding to the 3^{rd}, 5^{th}, 7^{th} and 9^{th} harmonic. With this information, it will be possible to change to a synchronous reference frame (dq) and use PI controllers to reduce its effect.

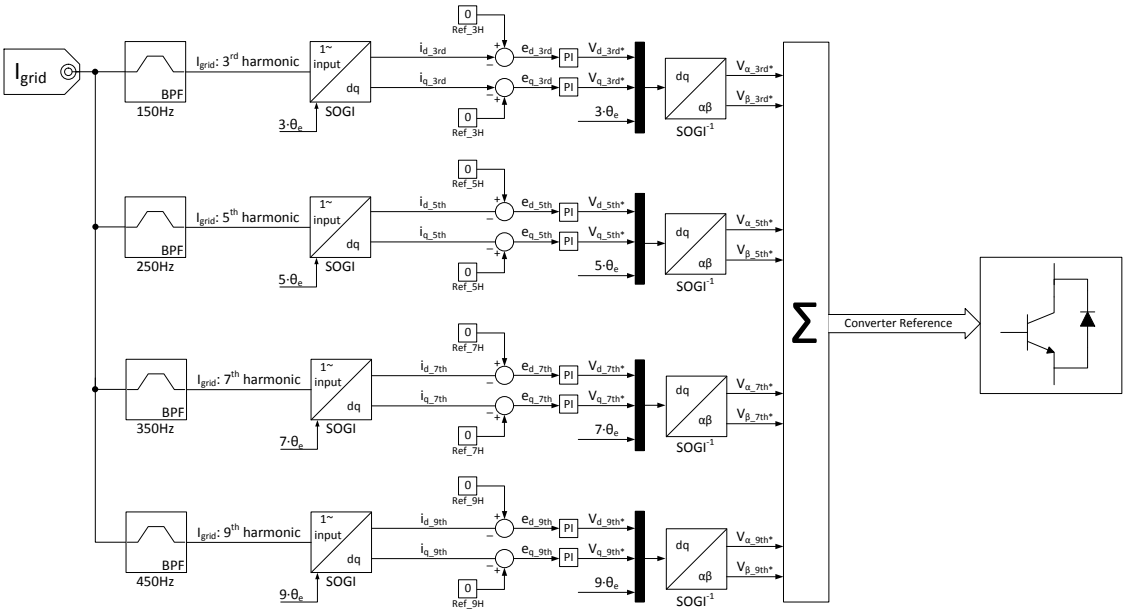

Figure 6-3: dq topology carried out to reduce the effect of the harmonics.

6.1.1 Unavailability of synchronous reference frame with BPF

As it is depicted in Figure 6-4a, the main drawback comes from the fact that with the BPF we can not obtain sinusoidal waveforms which make impossible to transform to

a *dq* reference frame due to the fact that the filter can not block the rest of frequencies quick enough.

In order to solve this issue, the BPF filters have been changed by Fast Fourier Transformations (FFT), that gives the responses shown in Figure 6-4b.

This solution is a bit tricky, because the computational cost that a FFT needs is much higher than using a BPF. So having four FFT working at the same time every simulation step will need a powerful CPU. In this case, the simulation has been done in a dSPACE, so the computational cost is not really a drawback. Nevertheless, in a real implementation, this topology may not be a good solution, but it is for a simulation. For a real implementation, the use of the Goertzel algorithm would be a better idea than a FFT, because the number of operations needed are much lower, thus the computational cost is also lower.

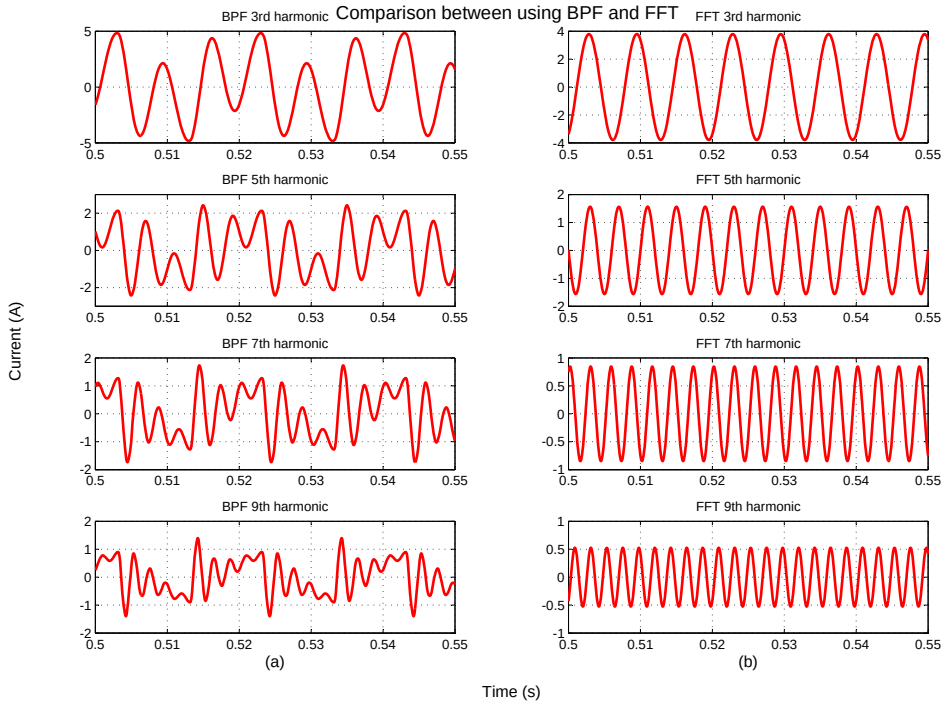

Figure 6-4: Difference of output harmonic selected current using a BPF or a FFT.

Table 6.1: Bandwidth chosen for the regulators

Bandwidth (Hz)	Harmonic frequency (Hz)
90	150
195	250
310	350
400	450

6.1.2 Control strategy

This control strategy was based on a previous work done during the first two months in Aalborg University. This scheme developed, called Grid Feeding, consists of being connected to the grid and inject the amount of d and q currents desired by the owner, always within the limits. Hence, the control strategy for harmonic compensation would be similar, but having current references equal to zero, as it can be seen in Figure 6-3.

In order to calculate the PI for a normal Grid Feeding connection, which means, inject current in the desired axis, but at 50Hz, the mathematical approach was based on the inductor and resistance of the output LC filter (and then improved with the dSPACE):

$$K_{pi} = 2 \cdot \pi \cdot bw \cdot L_f \tag{6.1}$$

$$K_{ii} = \frac{R_f}{L_f} \tag{6.2}$$

being bw the bandwidth of the controller, and, in this case, 1700Hz.

For the design of the high frequency regulators, the bandwidths have been chosen a bit lower of the respective frequency of the harmonic in order to keep the system stable. In Table 6.1 are summarized these values.

While the work was being carried out, an undesirable effect, called Whac-A-Mole, appeared. The correction of the different harmonics made another ones, which at the beginning were null, to show up..

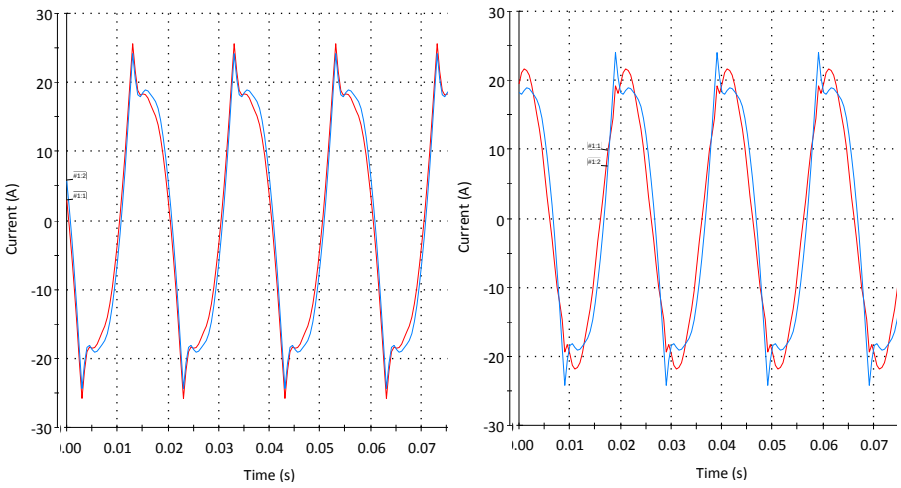

(a) Converter Off (b) Converter On

Figure 6-5: (a) Load (blue) and grid (red) current when the converter is off. (b) Load (blue) and grid (red) current when the converter is off.

6.1.3 Results

The results of the work are shown ahead. Since we have said that this topology was done previously in Simulink but adjusted in the dSPACE, we will show the results of the dSPACE and also prove we have worked with it.

In Figure 6-5 can be seen the difference of having the converter switched off or on. Figure 6-5a shows the real values of the current demanded by the loads. It can be appreciated the great amount of harmonics that this load can generate just by taking a brief look at the signal. When the converter is switched on, and after the setting time, the line current looks like the red signal of Figure 6-5b. Much more sinusoidal than the (a) case.

In order to prove what was said before, the THD of the line current will be shown now (Figure 6-6). It can be observed how the THD is reduced in more than a 15%.

It is also interesting to show some other results interesting from the point of view of power quality, like the value, in Amps, of the harmonic content of the line current before and after the use of the converter (Figure 6-7).

Finally, we will show how is the current delivered by the converter when it is trying to compensate the harmonic content of the line (Figure 6-8) and how does it

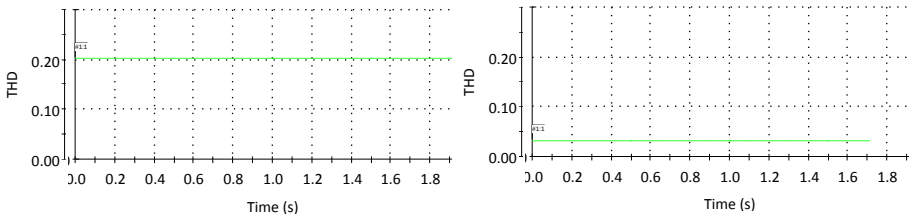

(a) Converter Off (b) Converter On

Figure 6-6: (a) THD of the line current when the converter is off. (b) THD of the line current when the converter is on.

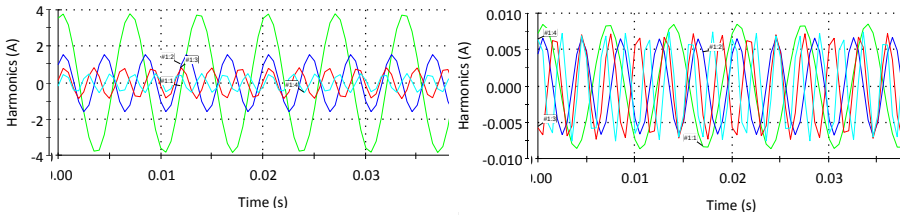

(a) Converter Off (b) Converter On

Figure 6-7: (a) Harmonics of the line current when the converter is off. (b) Harmonics of the line current when the converter is on.
Legend: Green: 3^{rd} harmonic. Blue: 5^{th} harmonic. Red: 7^{th} harmonic. Cyan: 9^{th} harmonic.

affect the grid frequency (Figure 6-9). It can be seen that it gives some ripple to the frequency but, even though it is not very high, it should be taken into account.

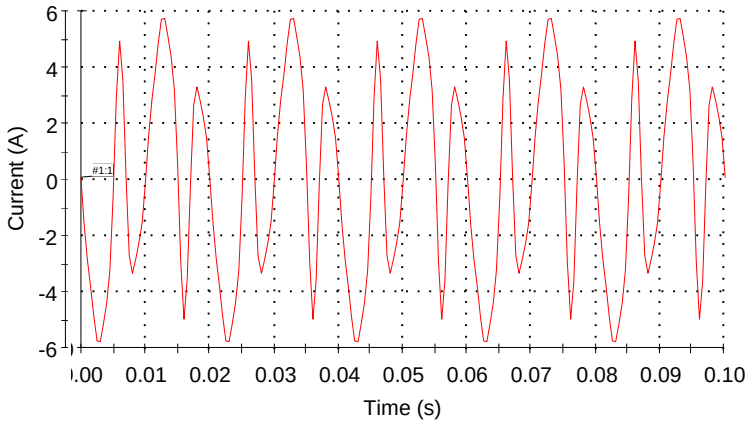

Figure 6-8: Current of the converter when is correcting the harmonic content.

6.2 Reduction of harmonic content in $\alpha\beta$ reference frame

The previously used topology is slightly seen in real world. Most of the works that can be found in the literature are carried out making use of Proportional-Resonant (PR) regulators [18], [19]. Thus this assertion, it has been developed a simulation to accomplish the same objective as in the previous case: reduce the effect of the harmonic content in a $\alpha\beta$ reference frame and using PR regulators. In addition, this simulation was done in Simulink and also with the dSPACE, but the results that will

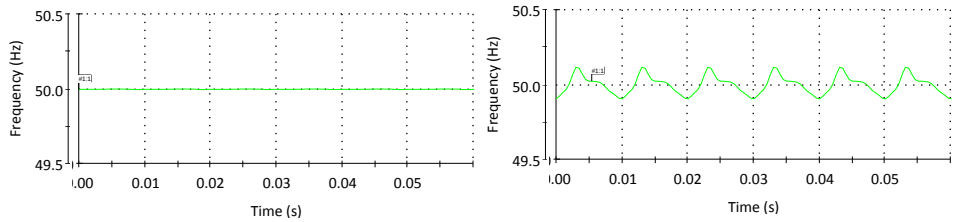

(a) Converter Off (b) Converter On

Figure 6-9: (a) Frequency of the grid calculated with a SOGI when the converter is off. (b) Frequency of the grid calculated with a SOGI when the converter is on.

be shown are from this last one.

6.2.1 Control strategy

As the power system is a single-phase one, the component β is useless, so the basic scheme changes lightly. In Figure 6-10 is shown the simplified control topology used in this simulation. A remarkable issue, comparing with the previous simulation in the

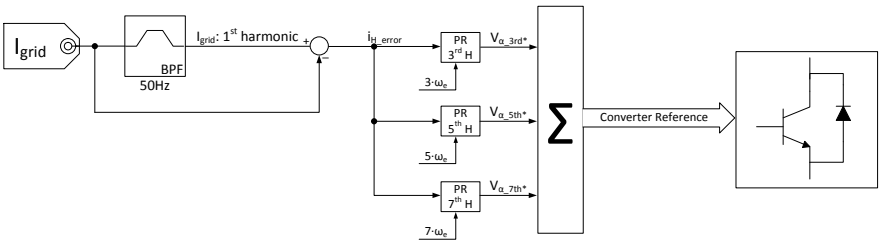

Figure 6-10: $\alpha\beta$ topology carried out to reduce the effect of the harmonics.

synchronous reference frame, is that in this case, a discrete resonant filter works fine when the 50Hz component of the line current needs to be extracted and no FFT had to be used. Since this scheme is based on a CM-VSI Grid Feeding in $\alpha\beta$ reference frame, there is only a current loop, so the closed-loop transfer function would be:

$$v_c = \left(\frac{-1 \,/\, C_s}{LCs^2 + (C_s G_i(s) G_{PWM}) + 1} \right) i_o \tag{6.3}$$

and the transfer function of a PR current controller is:

$$G_i(s) = k_{pI} + \frac{k_{iI} s}{s^2 + 2\omega_c s + \omega_o^2} \tag{6.4}$$

But, as the main point is reducing the harmonic effect, then the PR regulators that will be used only will consist of a resonant component, because the proportional one would make unstable the system.

$$G_{iH}(s) = \sum_{h=3,5,7} \frac{k_{IHh} s}{s^2 + 2\omega_c s + (\omega_o h)^2} \tag{6.5}$$

Instead of using the Matlab functions "bode" or "rltools", we have designed the resonant regulators with the dSPACE. Due to resonances in the circuit, trying to correct the 7^{th} harmonic provokes a great disturbance in the 3^{rd} and 5^{th} resonant controllers. Hence the only harmonics able to correct were these two ones. The study of the correction of also the 7^{th} harmonic will be done in Section 6.2.3.

6.2.2 Results

The results of the work are shown ahead. We will illustrate how the harmonics 3 and 5 are reduced but not the 7^{th} or higher. Nevertheless, the THD has been reduced in almost a 15%, which is a noticeable value.

With the previous simulation, the most remarkable issue that should be mentioned is the final THD value, that finishes being a bit lower in the dq case than in the $\alpha\beta$. On the other hand, the computational cost is lower in the stationary reference frame topology, because it does not need any FFT.

In Figure 6-11 can be seen the difference of having the converter switched off or on. Figure 6-11a shows the real values of the current demanded by the loads. When the converter is switched on, the line current looks like the red signal of Figure 6-11b. Much more sinusoidal than the (a) case and with a lower THD, as we will see ahead. In order to prove what was said before, the THD of the line current will be shown now (Figure 6-12). It can be observed how the THD is reduced in a 15% even though the 7^{th} harmonic has not been corrected.

From the point of view of power quality, it is shown now, in Amps, the harmonic content of the line current before and after the use of the converter (Figure 6-13).

Finally, we will show how the current is delivered by the converter when it is trying to compensate the harmonic content of the line (Figure 6-14) and how it does affect the grid frequency (Figure 6-15). It can be seen that it gives some ripple to the frequency but, even though it is not very high, it should be taken into account.

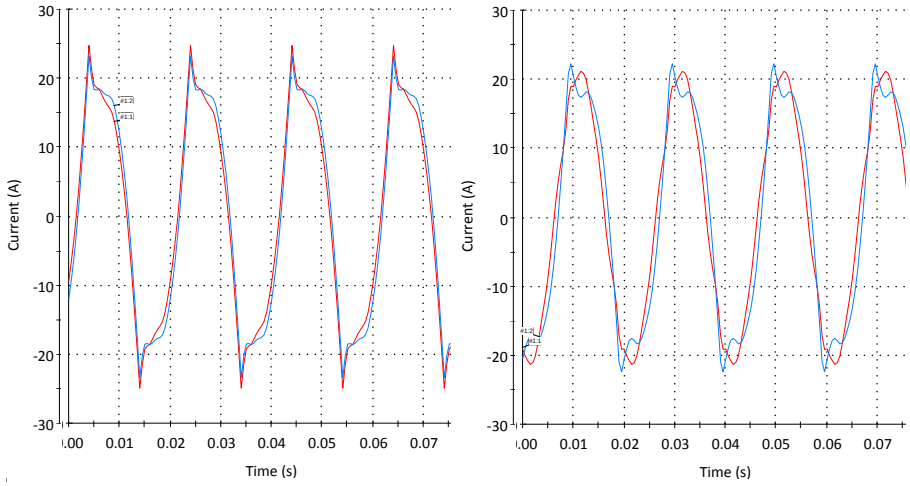

(a) Converter Off (b) Converter On

Figure 6-11: (a) Load (blue) and grid (red) current when the converter is off. (b) Load (blue) and grid (red) current when the converter is off.

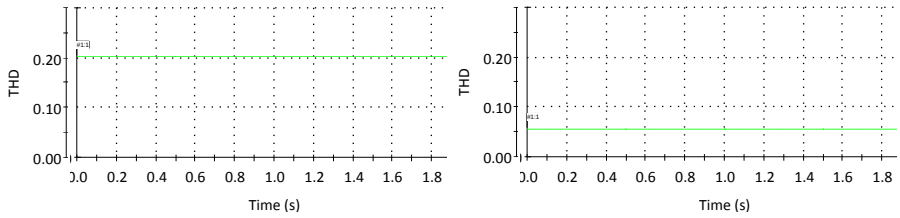

(a) Converter Off (b) Converter On

Figure 6-12: (a) THD of the line current when the converter is off. (b) THD of the line current when the converter is on.

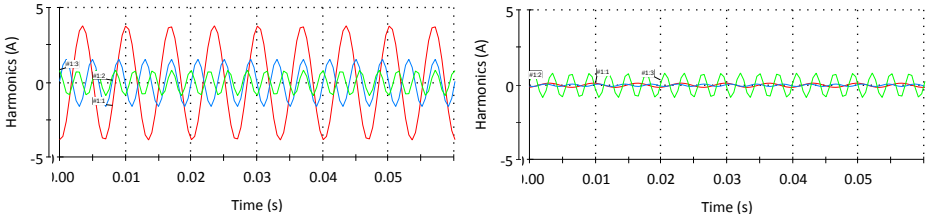

(a) Converter Off (b) Converter On

Figure 6-13: (a) Harmonics of the line current when the converter is off. (b) Harmonics of the line current when the converter is on.
Legend: Red: 3^{rd} harmonic. Blue: 5^{th} harmonic. Green: 7^{th} harmonic.

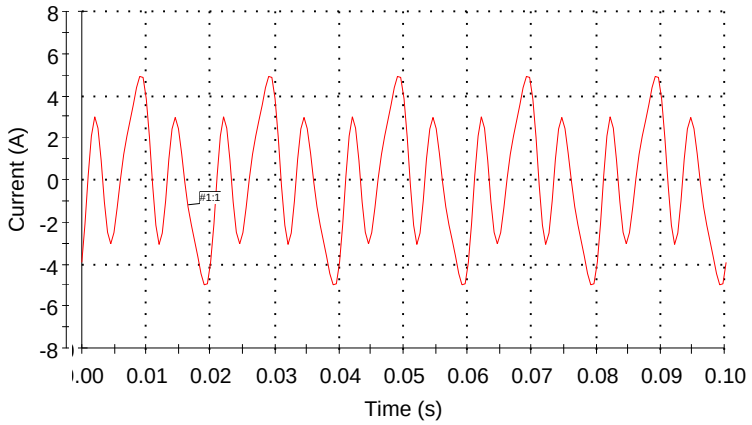

Figure 6-14: Current of the converter when is correcting the harmonic content.

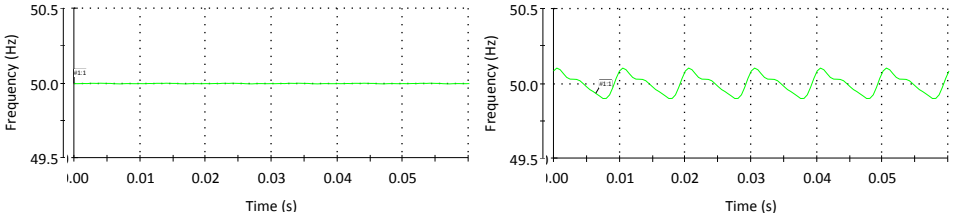

(a) Converter Off (b) Converter On

Figure 6-15: (a) Frequency of the grid calculated with a SOGI when the converter is off. (b) Frequency of the grid calculated with a SOGI when the converter is on.

6.2.3 Correction of the 7^{th} harmonic

As it was said before, due to resonance issues, correcting the 7^{th} harmonic was impossible, despite of any combination of regulators for the lower harmonics. Nevertheless, changing the output inductor of LCL filter that connects the grid with the converter, a possible regulation of the 350Hz component appears. By reducing the inductor from $1.8mH$ to $0.18mH$, the correction of the harmonic content stays as follows in Figure 6-19.

The current that the grid supplies to the load is lower and with less high frequency content, like it can be seen in Figure 6-16.

On the other hand, and unlike the previous cases, the frequency (Figure 6-17) of the whole system is not affected after the converter is switched on.

And finally, the converter current is shown ahead (Figure 6-18).

The THD of the current given by the grid is reduced to a value of 4.05%, where the

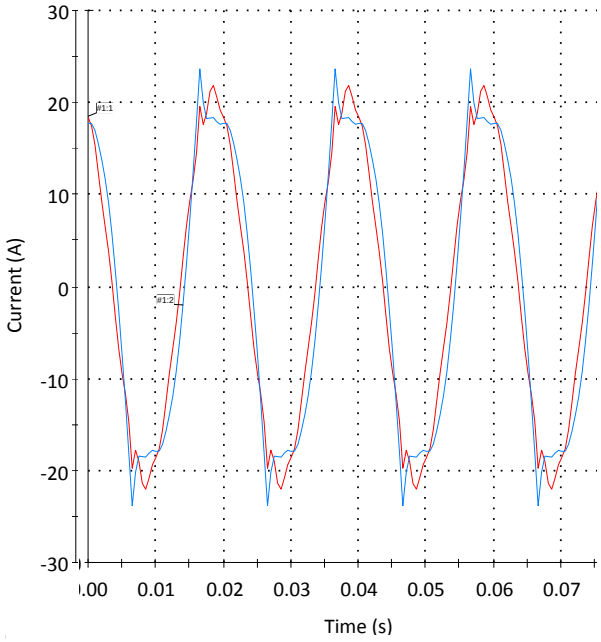

Figure 6-16: Load (blue) and grid (red) current.

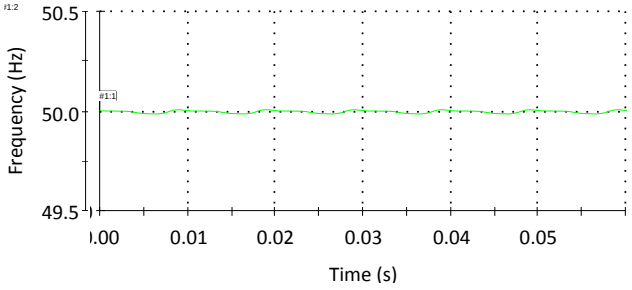

Figure 6-17: Grid frequency.

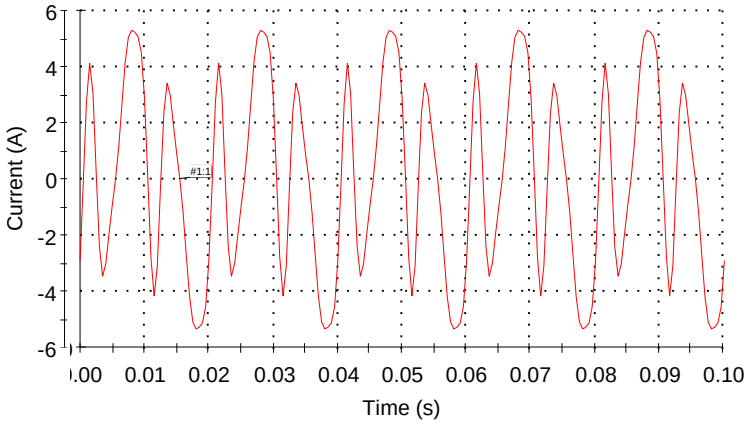

Figure 6-18: Current of the converter when is correcting the harmonic content.

harmonic content can be seen in Figure 6-19, in % with respect of the fundamental.

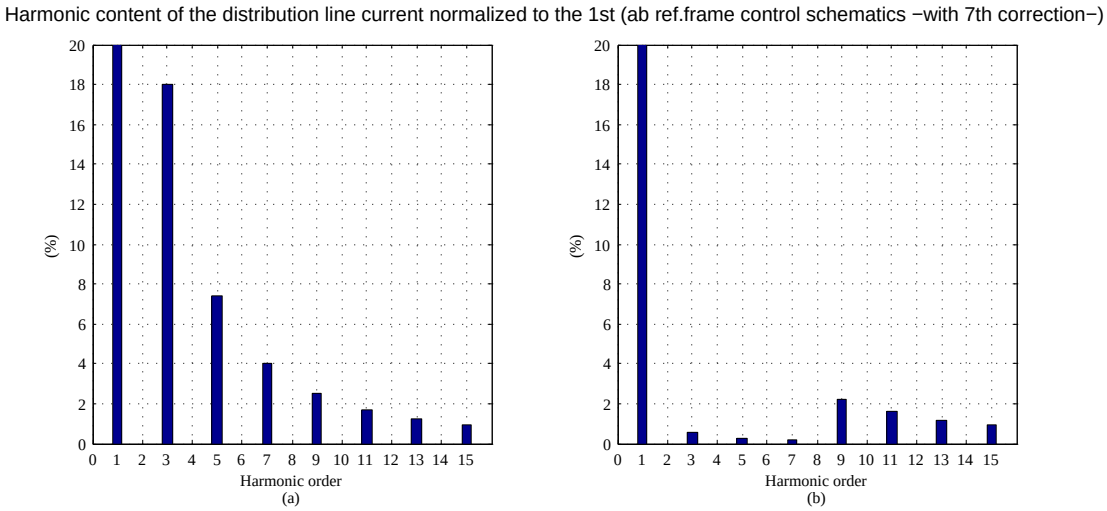

Figure 6-19: Harmonic content when the converter is off and on ($\alpha\beta$ ref. frame with 7^{th} harmonic correction).

6.3 Final comparison between both topologies

In order to see together the final results, the harmonic content, before and after switching on both converters in synchronous (Fig. 6-20) and stationary (Fig. 6-21) reference frame will be shown. It can be seen that the converter which uses $\alpha\beta$ coordinates is not able to reduce the harmonic content as much as the dq one. The other great difference is the order of the harmonics: in the stationary reference frame, as we could not correct the 7^{th} and higher components (without modifying the LCL filter), they remain as at the beginning. Nevertheless, in the synchronous reference frame, all the lower harmonics can be almost completely deleted. The values shown are normalized to the 1^{st} harmonic and in %.

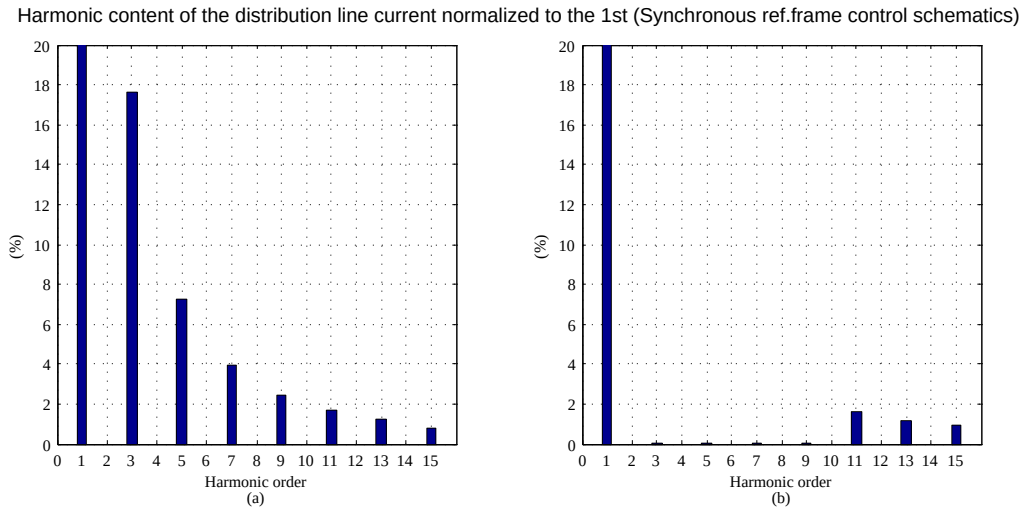

Figure 6-20: Harmonic content when the converter is off and on (dq ref. frame).

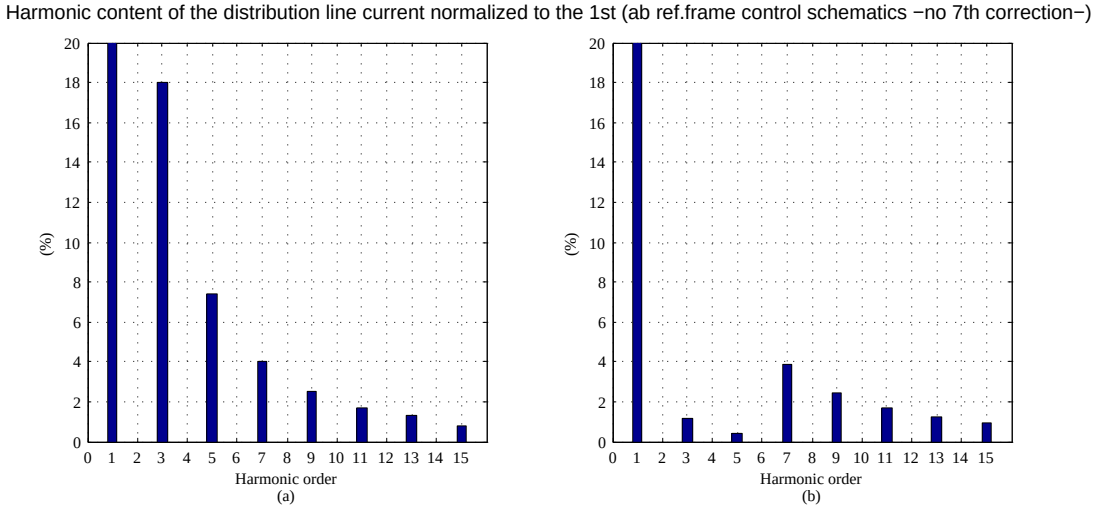

Figure 6-21: Harmonic content when the converter is off and on ($\alpha\beta$ ref. frame without 7^{th} harmonic correction).

Chapter 7

Conclusions

This master thesis has illustrated a methodology to improve the THD of a distribution line configuration with multiple non-linear loads, by measuring only the voltage at the PCC, thus avoiding the use of current measurement. The effect on the distribution line current distortion of such loads, represented by a group of lampposts with their respective LF ballasts and the HPS lamps is shown, mainly in the 3^{rd}, the 5^{th} and the 7^{th}harmonics of the line current and in the current THD. The proposed configuration has reduced significantly those harmonics and also the final THD. More in deep work should be done to elucidate the real effect of the gain K_1 and an exhaustive analysis of the dynamics of the whole system has to be carried out. As it was mentioned before, the bigger the value of this gain, the better the THD of the line current, but physically is impossible to achieve an infinite value, so we need a compromise within the simulation values and the feasible ones. On the other hand, we have demonstrated that there are other topologies to correct the harmonic content of the current, but they need current measurements, that are the ones we are trying to avoid. These different control schemes carried out, in stationary and in synchronous reference frame, have shown very good results but with some differences between them, as it was mention in Chapter 6.

Chapter 8

Future developments

In this simulation, the converter was represented by a current source. In the future, it will be implemented using an H-bridge due to the fact that active and reactive powers have to be fully decoupled. The increase of distributed generation on electric networks has raised the concern of grid stability, among other issues. In this Master Thesis, grid stability was not analyzed hence it will be taken into account in future papers and researches. The proposed control has the needed tools to achieve a total control of the demanded line current, thus implementing more functionalities should not suppose great difficulties. The development of the control was done by supposing the load is known though it does not happen in real life. Future works will include an algorithm to estimate the loads and adapt the controller in its function. Furthermore, the controller could be designed as a PI and look for zero steady-state error.

It is important to remind that FFT have been used in a control schematics developed in this work. These FFT should be change by Goertzel algorithm, which would reduce the number of calculations needed.

There is also room for improvement in the lamp model. It should be tested in other operating conditions, as the starting point, the warm-up time or during its ageing.

The final stage would be implement this topology with real elements and check its behavior during enough time to ensure it works and does not become unstable.

Chapter 9

Quality report

Writing this master thesis abroad it has been a great opportunity to develop my skills working in a new researching group. I have learnt many new things, like topologies and techniques used in single-phase systems, that will be useful for my PhD or in my future career. I strongly recommend the following master students to go out of Spain and see how people work around the world. They will meet new fellows and will know to work a bit more autonomously, which is important if you don't want to depend always on someone. On the other hand, I think there is enough time to write this thesis and if its quality does not match with the one demanded, I do not really know what should be done. I suppose it depends on the case. My concrete case was successful and I have absolutely no regrets.

Chapter 10

Work done as a guest in Aalborg University

This Master Thesis has been based on a paper send to IECON 2013, so part of the work was developed in Spain and part in Denmark. Chapter 6 was done completely in Aalborg University, at the Department of Energy Technology (Power Electronic Systems), among other simulations that had no point to be included in this work but that will be explained ahead:

The first two months we have been doing several simulations of converters working connected to the grid and in island mode, with and without droop and in a synchronous reference frame. From now on, we will also do these simulations again but in a stationary reference frame, which means using PR regulators.

For this thesis, both harmonic correction converters were done (chapter 6), using PI and PR regulators.

Now, having these control schemes working, we can do more complex simulations, putting together different types of converters and also going further implementing them in real devices. We have been asked to try to connect single-phase converters to three-phase microgrids and see how it helps to compensate and balance that local grid.

Bibliography

[1] *Climate TechBook: Residential and Commercial Sectors Overview*, 2009

[2] Branas, C.; Azcondo, F.J.; Bracho, S., "Evaluation of an electronic ballast circuit for HID lamps with passive power factor correction," IECON 02 [Industrial Electronics Society, IEEE 2002 28th Annual Conference] , vol.1, no., pp.371,376 vol.1, 5-8 Nov. 2002

[3] Nyland, F.; Schlichting, L. C M; Liz, M. B.; Raizer, A., "Analysis of harmonic distortion and electromagnetic interference due to and electromagnetic ballasts," Harmonics and Quality of Power, 2002. 10th International Conference on , vol.2, no., pp.765,769 vol.2, 6-9 Oct. 2002

[4] Rico-Secades, M.; Corominas, E.L.; Alonso, J.M.; Ribas, J.; Cardesin, J.; Calleja, A.J.; Garcia-Garcia, J., "Complete low-cost two-stage electronic ballast for 70-W high-pressure sodium vapor lamp based on current-mode-controlled buck-boost inverter," Industry Applications, IEEE Transactions on , vol.41, no.3, pp.728,734, May-June 2005

[5] Dalla Costa, M.A.; Alonso, J.M.; Garcia-Garcia, J.; Cardesin, J.; Ribas, J., "Analysis, Design and Experimentation of a Closed-Loop Metal Halide Lamp Electronic Ballast," Industry Applications Conference, 2006. 41st IAS Annual Meeting. Conference Record of the 2006 IEEE , vol.3, no., pp.1384,1390, 8-12 Oct. 2006

[6] Singh, Bhim; Al-Haddad, K.; Chandra, A., "A review of active filters for power quality improvement," Industrial Electronics, IEEE Transactions on , vol.46, no.5, pp.960,971, Oct 1999

[7] Enjeti, P.; Shireen, W.; Pitel, I., "Analysis and design of an active power filter to cancel harmonic currents in low voltage electric power distribution systems," Industrial Electronics, Control, Instrumentation, and Automation, 1992. Power Electronics and Motion Control., Proceedings of the 1992 International Conference on , vol., no., pp.368,373 vol.1, 9-13 Nov 1992

[8] Rodriguez, A.; Giron, C.; Saez, V.; Rizo, M.; Bueno, E.; Rodriguez, F.J., "Analysis of repetitive-based controllers for selective harmonic compensation in active power filters," IECON 2010 - 36th Annual Conference on IEEE Industrial Electronics Society , vol., no., pp.2013,2018, 7-10 Nov. 2010

[9] Newman, M.J.; Holmes, D.G., "A universal custom power conditioner (UCPC) with selective harmonic voltage compensation," IECON 02 [Industrial Electronics Society, IEEE 2002 28th Annual Conference] , vol.2, no., pp.1261,1266 vol.2, 5-8 Nov. 2002

[10] Fujita, H.; Yamasaki, T.; Akagi, H., "A hybrid active filter for damping of harmonic resonance in industrial power systems," Power Electronics, IEEE Transactions on , vol.15, no.2, pp.215,222, Mar 2000

[11] Savaghebi, M.; Jalilian, A.; Vasquez, J.C.; Guerrero, J.M., "Selective compensation of voltage harmonics in an islanded microgrid," Power Electronics, Drive Systems and Technologies Conference (PEDSTC), 2011 2nd , vol., no., pp.279,285, 16-17 Feb. 2011

[12] Rahman, N.F.A.; Hamzah, M.K.; Noor, S.Z.M.; Hasim, A.S.A., "Single-phase hybrid active power filter using single switch parallel active filter and simple passive filter," Power Electronics and Drive Systems, 2009. PEDS 2009. International Conference on , vol., no., pp.40,45, 2-5 Nov. 2009

[13] Moo, C.S.; Chuang, Y.C.; Lee, J.C., "A new dynamic filter for the electronic ballast with the parallel-load resonant inverter," Industry Applications Conference, 1995. Thirtieth IAS Annual Meeting, IAS '95., Conference Record of the 1995 IEEE , vol.3, no., pp.2597,2601 vol.3, 8-12 Oct 1995

[14] Torrey, D.A.; Al-Zamel, A.M.A.M., "Single-phase active power filters for multiple nonlinear loads," Power Electronics, IEEE Transactions on , vol.10, no.3, pp.263,272, May 1995

[15] Lavopa, E.; Zanchetta, P.; Sumner, M.; Bolognesi, P., "Improved voltage harmonic control for sensorless shunt active power filters," Power Electronics Electrical Drives Automation and Motion (SPEEDAM), 2010 International Symposium on , vol., no., pp.221,226, 14-16 June 2010

[16] Buso, S.; Malesani, L.; Mattavelli, P., "Comparison of current control techniques for active filter applications," Industrial Electronics, IEEE Transactions on , vol.45, no.5, pp.722,729, Oct 1998

[17] Wojciechowski, D., "Grid voltages sensorless control system of the PWM rectifier with active filtering function," Compatibility in Power Electronics, 2005. IEEE , vol., no., pp.238,246, June 1, 2005

[18] Micallef, A.; Apap, M.; Spiteri-Staines, C.; Guerrero, J.M., "Cooperative control with virtual selective harmonic capacitance for harmonic voltage compensation in islanded microgrids," IECON 2012 - 38th Annual Conference on IEEE Industrial Electronics Society , vol., no., pp.5619,5624, 25-28 Oct. 2012

[19] Briz, F.; Diaz-Reigosa, D.; Degner, M.W.; Garcia, P.; Guerrero, J.M., "Dynamic behavior of current controllers for selective harmonic compensation in three-phase active power filters," Energy Conversion Congress and Exposition (ECCE), 2011 IEEE , vol., no., pp.2892,2899, 17-22 Sept. 2011

[20] Wei Yan; Hui, S.Y.R., "A universal PSpice model for HID lamps," Industry Applications, IEEE Transactions on , vol.41, no.6, pp.1594,1602, Nov.-Dec. 2005

[21] Sanchez, R.O.; Vazquez, N.; Hernandez, C.; Rodriguez, E.; Pinto, S.; Juarez, M., "Electric Dynamic Modeling of HID Lamps for Electronic Ballast Design," Industrial Electronics, IEEE Transactions on , vol.57, no.5, pp.1655,1662, May 2010

[22] Wang Wei; Zhu Guo-dong; Xu Dian-guo, "A physics-based model for HID lamps with rectifying effect," Vehicle Power and Propulsion Conference, 2008. VPPC '08. IEEE , vol., no., pp.1,5, 3-5 Sept. 2008

[23] Guerrero, J.M.; Vasquez, J.C.; Teodorescu, R.; Kerekes, T., "Industrial/PhD course on Microgrids in Theory and Practice," Aalborg University. Nov. 2012

[24] De Brabandere, K., Doctoral Thesis: Voltage and frequency droop control in low voltage grids by distributed generators with inverter front-end

I would like to thank all the people who made this Master Thesis possible: my professors, especially Jorge, whose patience reached critical levels during the correction of the paper, first, and the thesis later; Pablo García, who helped to develop the mathematical model and in many other things that are impossible to describe; Pablo Arboleya, who was the first to teach me how to work with microgrids, something that I took advantage of during my stay in Aalborg and also the one who push me to use LaTex; and finally, thanks to Josep and his team for giving me the opportunity of work in their lab and make me feel like one more of their group. I can't leave without thanking my family and my girlfriend for being there to hear my laments when something didn't work. Maybe you guys didn't notice, but I appreciated it so much.